

# USE OF CFD TO PREDICT CRITICAL HEAT FLUX IN ROD BUNDLES

**Z. E. Karoutas, Y. Xu, L. David Smith, III, P. F. Joffre, Y. Sung\***

Westinghouse Electric Company  
5801 Bluff Rd, Hopkins, SC 29061

[karoutze@westinghouse.com](mailto:karoutze@westinghouse.com); [xuy@westinghouse.com](mailto:xuy@westinghouse.com); [smith1ld@westinghouse.com](mailto:smith1ld@westinghouse.com)  
[joffrepf@westinghouse.com](mailto:joffrepf@westinghouse.com); [sungy@westinghouse.com](mailto:sungy@westinghouse.com)

## ABSTRACT

A high fidelity Computational Fluid Dynamics (CFD) tool which can predict critical heat flux (CHF) is being developed, so that PWR fuel assembly spacer grid designs can be optimized prior to performing expensive CHF testing. This paper presents an example of CFD-based CHF modeling development of a fuel component design with comparison to available test data. Westinghouse has performed 5x5 rod bundle tests for many spacer grid designs with and without mixing vanes where Laser Doppler Velocimeter (LDV), pressure drop, single phase subchannel mixing and CHF test data exist to support CFD tool validation. The Star-CCM+ CFD code was used to prepare the models and run cases to compare to available test data.

## KEYWORDS

CFD, CHF, LDV, Rod Bundle, Mixing

## 1. INTRODUCTION

Critical Heat Flux (CHF), also referred to as DNB (Departure from Nucleate Boiling), is an important parameter in the design and operation of nuclear fuel and nuclear plants. From 1963 until 2003, all the CHF test data, which formed the basis for Westinghouse CHF correlations licensed in the US, were obtained from the Heat Transfer Research Facility (HTRF) of Columbia University in New York City. After HTRF's permanent closure in 2003, Westinghouse built its own new CHF test facility: ODEN. ODEN loop qualification testing versus HTRF was completed in 2010 [1]. ODEN has been used for rod bundle CHF and mixing tests in support of PWR applications since. However, CHF tests of PWR fuel designs are costly and require lengthy preparation time. In order to evaluate the CHF performance of a new grid spacer design, the grids have to be manufactured, assembled, and shipped to the test location. CFD codes with a single phase heat transfer model have been previously used in selecting grid design for CHF performance. However, the presence of the boiling and the steam can change the fuel rod heat transfer significantly. Without the proper 2-phase boiling model, CFD simulations could create misleading results. The single and 2-phase models in the CFD tool need to be validated with the test data applicable to the PWR fuel design.

To support validation, the CFD model results were compared to LDV data from 5x5 rod bundle tests for a spacer grid design. The CFD predictions were then compared to 5x5 rod bundle single phase mixing data where exit subchannel temperature measurements were compared to predictions for grids with and without mixing vanes. After confirming the CFD tools make reasonable predictions for velocity profiles and exit subchannel temperatures, an approach to predicting CHF using the available two-phase flow boiling models in Star-CCM+ for the PWR rod bundle has been developed for comparison to CHF test data.

---

\* ©2015 Westinghouse Electric Company LLC, All Rights Reserved

## 2. DESCRIPTION OF TEST DATA FOR CFD VALIDATION

Rod bundle tests were performed in a 5x5 rod array to support CFD tool validation. These tests included exit subchannel temperature measurements to confirm subchannel mixing, LDV measurements to confirm velocity profiles, and CHF measurements to confirm CHF predictions. These tests are described in the following sections.

### 2.1. Exit Subchannel Temperature Tests

Two 5x5 rod bundle tests were performed to measure subchannel temperatures at the end of the test section. These tests utilize a 5x5 rod array, uniform axial power shape, equivalent rod radial power distribution and a power split between hot and cold rods of ~1.2. Two different grid designs were tested; one with mixing vanes (MV) and the other without mixing vanes (NMV). The mixing vane design used in these tests is a split vane type in each subchannel where an alternating swirling flow pattern and crossflow mixing are produced in adjacent subchannels. Figures 1 and 2 describe the radial and axial geometries for these 5x5 tests. Figures 3 and 4 provide a visual description of the non-mixing and mixing vane spacer grids used in the tests. The exit subchannel thermocouples are located at the center of each subchannel. Type K, 0.040 inch thermocouples were used. Approximately 30 single phase tests were run for each rod bundle geometry, covering a wide range of operating conditions; flow, pressure and inlet temperature.

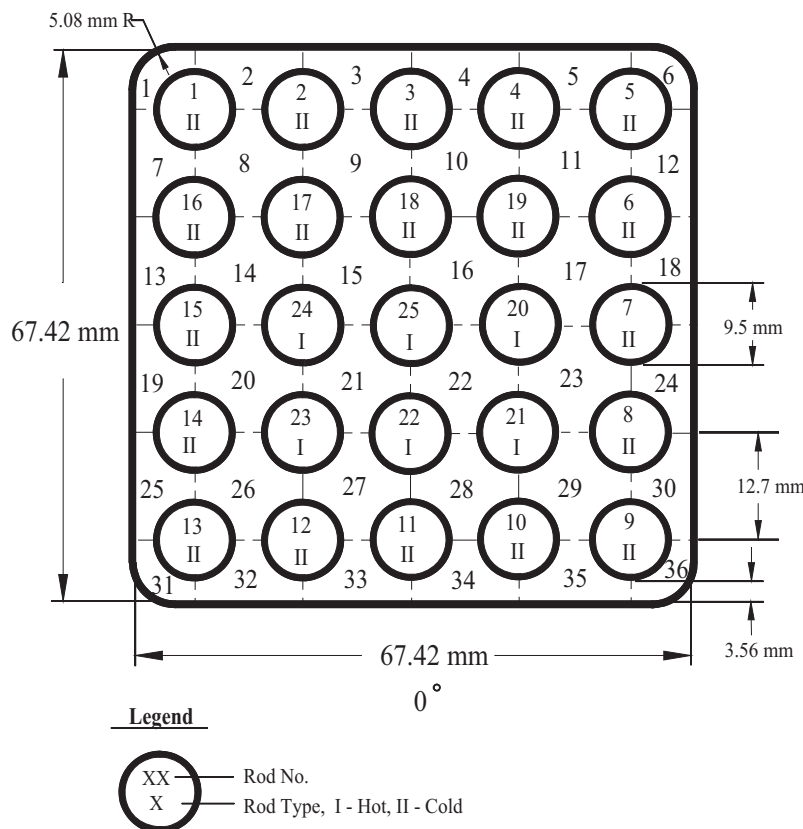


**Figure 1 Radial Geometry of 5x5 Mixing Tests**

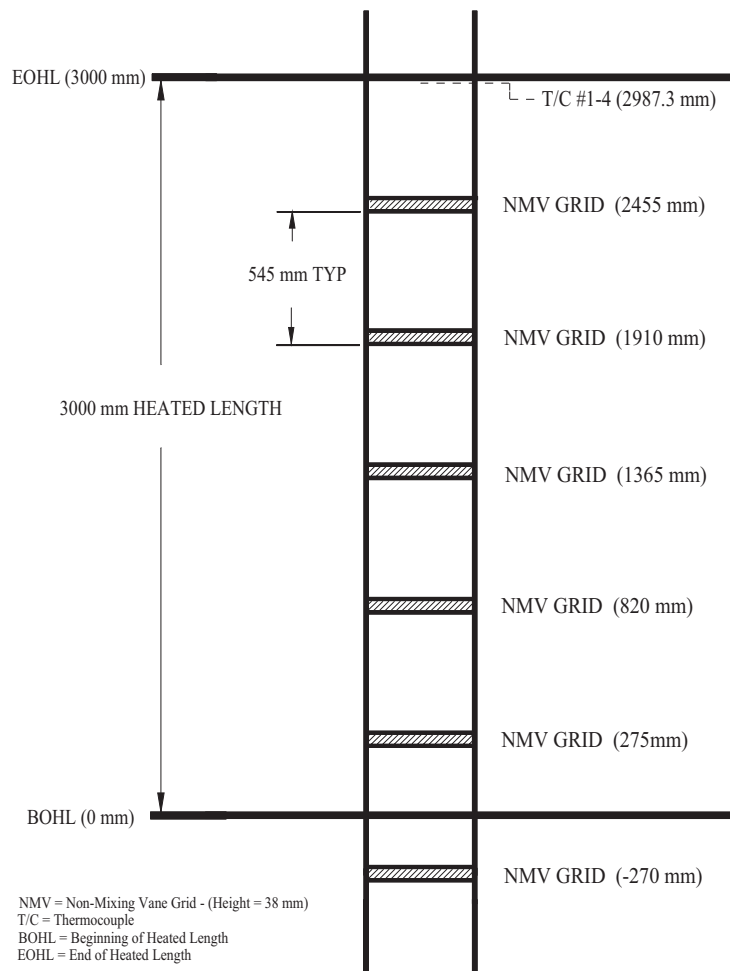


**Figure 2 Axial Geometry for 5x5 Mixing Tests (NMV or MV grids)**

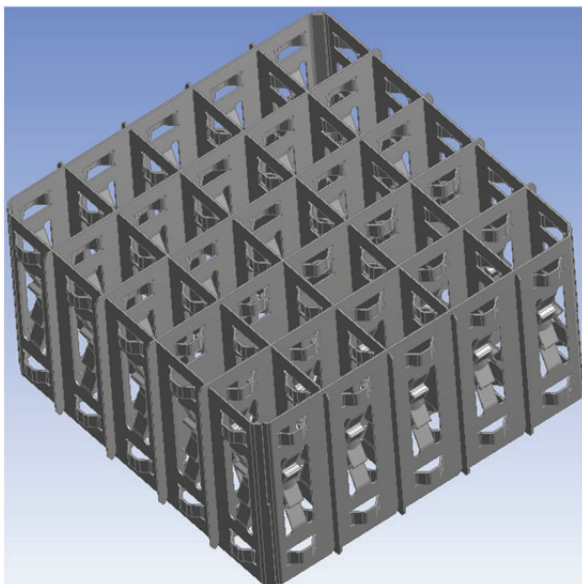


**Figure 3 Non-Mixing Vane Grid Geometry**

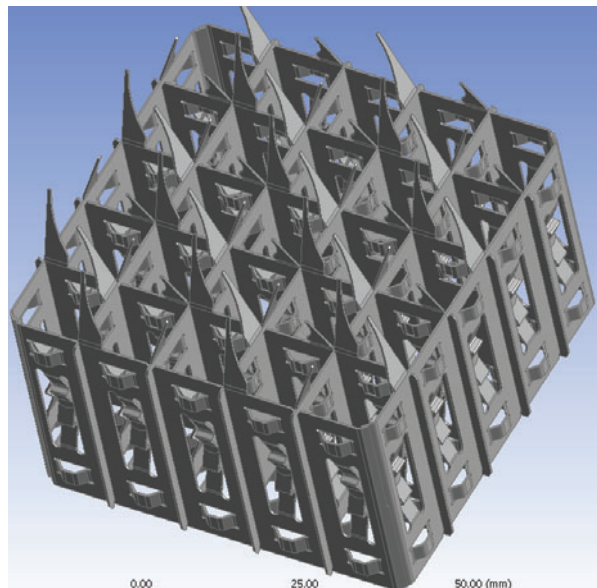


**Figure 4 Mixing Vane Grid Geometry**

## 2.2. Laser Doppler Velocimeter Tests

LDV tests were performed on a similar 5x5 split vane mixing grid type used in the tests described in Section 2.1. Figures 5 and 6 describe the radial and axial geometries of the 5x5 LDV tests where axial and lateral LDV measurements were made from one side through the center of the subchannels at several axial levels downstream of the grid. These tests were performed at cold flow conditions.

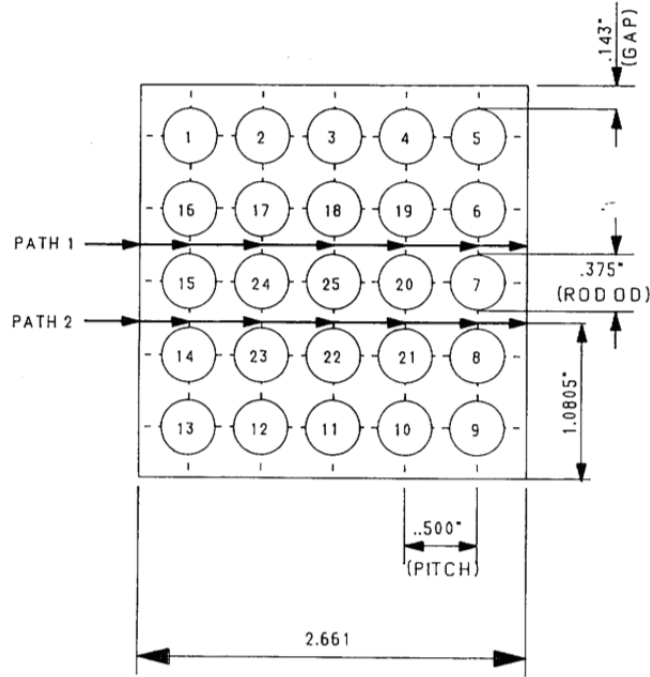


Figure 5 Radial Geometry of LDV Measuring Paths

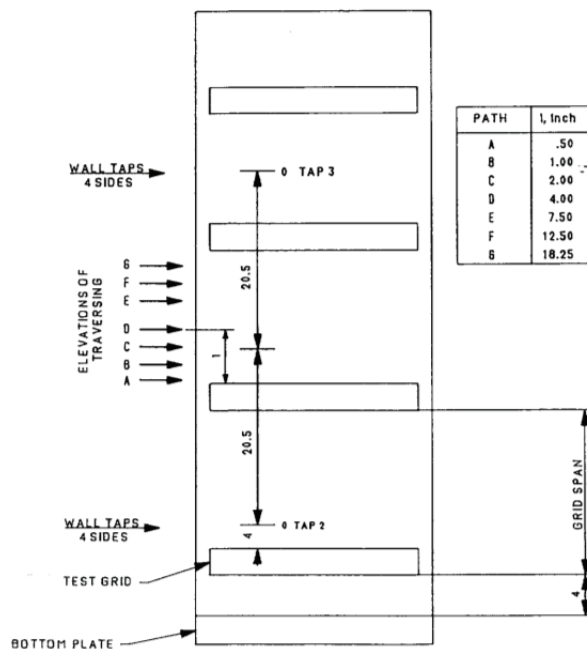


Figure 6 Axial Geometry of LDV Measuring Paths

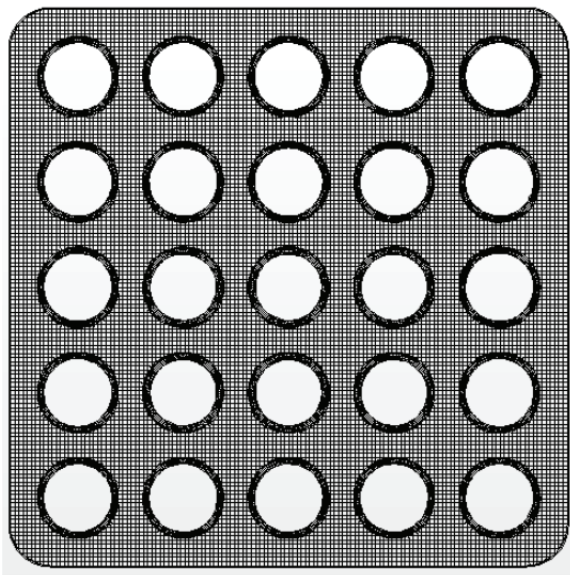
### 2.3. Critical Heat Flux Tests

CHF tests were performed for a 5x5 rod array with mixing vane and non-mixing vane grid [2]. Figures 1 and 2 describe the radial and axial geometries for the CHF tests. Figures 3 and 4 show the grids used in the tests. These tests utilized a uniform axial power shape, similar rod radial power distribution, with no simulated thimble. The power split between hot and cold rods is  $\sim 1.2$ . Typically, approximately 100 CHF points were obtained in each test covering a wide range of thermal hydraulic operating conditions that a reactor could reach. The following is a brief description on the process for obtaining a CHF point.

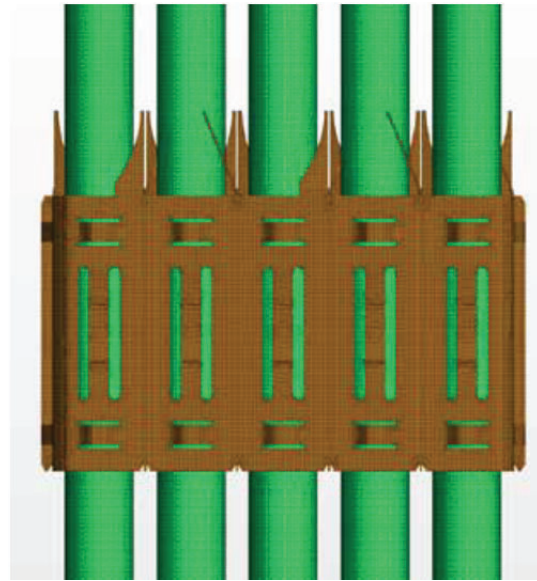
First, the desired steady state condition at the test section was established with respect to flow, exit pressure, and inlet temperature. The initial power applied to the test bundle was about 20 percent below that corresponding to the expected CHF power level at that condition. Once the set point was established, the CHF condition was approached in the quasi-steady state manner. While flow and pressure were held constant and with inlet temperature held constant via heat exchanger control, the bundle power was slowly and manually increased in small increments ( $\leq 30$  kW) until a temperature excursion was observed in one (or more) TCs in the heater rods.

### 3. DEVELOPMENT OF CFD MODELS

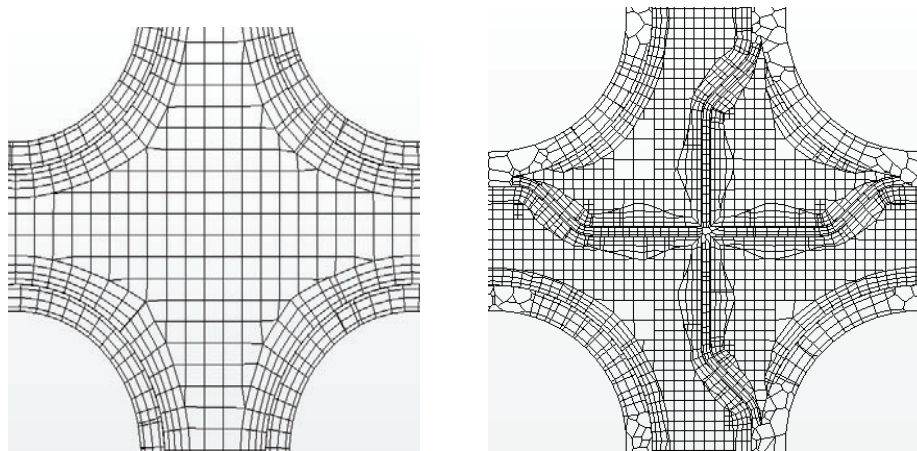
CFD models were prepared for the rod bundle tests using the Star-CCM+ CFD code [3]. CFD analyses were performed to predict the measured exit subchannel temperatures and velocity profiles in single phase flow. The CFD model domain represents the exact geometry in the test loop from the beginning of the heated length to the end of the heated length. A detailed hexahedral dominant mesh shown in Figure 7 was used in the CFD model. The initial CFD model development was performed in Reference [2]. Total number of cells in the model was  $\sim 145$  million. The base size of 0.6 mm was chosen with four layers of a prism layer created next to solid surfaces from mesh sensitivity study experience. The thickness of the first prism layer was chosen so that majority of  $y^+$  values on the rods is larger than 30. A thin mesher was used for cladding mesh of 4 layers in solid. The Quadratic K epsilon turbulence model with the default coefficients and the high  $y^+$  wall treatments was used in the analysis. The CFD models for both grids were run at the similar thermal hydraulic boundary conditions.



(a) Mesh in Cutting Plane



(b) Mesh on the Grids and Rods



(c) Zoomed Mesh in Cutting Plane

(d) Zoomed Mesh on the Grids and Rods

**Figure 7 Mesh for CFD Model**

To predict the onset of DNB, CFD analysis was performed with the Star-CCM+ CFD code version 7.06.012. Two-phase flow CFD analyses were performed using the customized nucleate boiling model. The 2-fluid boiling model in StarCCM+ outlined by Lo [4] including a description of the equations was used. The Eulerian-Eulerian two-phase model where both phases coexist everywhere in the flow domain was employed in the model. The interfacial drag force is critical for the bubble distribution in the domain. The drag coefficient was computed according to Tomiyama [5] for a contaminated fluid system. The Wall boiling model was used to calculate the heat transfer near the wall. The evaporation heat flux in the wall boiling model was determined by the nucleation density and the bubble departure diameter. The nucleation site density was calculated based on the formula developed by Lemmert and Chawla [6]. The bubble departure diameter was based on Tolubinsky and Kostanchuk [7]. The bubble size distribution was based on the method developed by Kurul and Podowski [8] in which a linear function is applied between measured (predicted) bubble diameters at two specified values of liquid sub-cooling. It shall be mentioned that the partition wall boiling model was not specifically developed for the current conditions, particularly missing the heat transfer mechanism due to bubble sliding on surfaces. A more appropriate model developed by Gilman [14] with a more advanced wall partitioning can improve the heat transfer modeling compared to the classic Kurul and Podowski model.

#### **4. COMPARISON OF CFD PREDICTIONS TO TEST DATA**

The CFD predictions were compared to the 5x5 rod bundle test data in the following sections.

##### **4.1. Comparisons to Exit Subchannel Temperature Data**

Figures 8 & 9 show the flow patterns in the subchannels ~ 1 hydraulic diameter downstream of the grids. The mixing vane grid showed an alternating swirling flow pattern in the subchannels but the non-mixing vane grid showed no swirl. The CFD results [9] show that the mixing vanes promote strong coolant movement between the fuel rod surface and the channel center. To demonstrate the temperature profile at the end of the heated length where subchannel temperature measurements were obtained at the center of each subchannel, the CFD coolant temperature distributions are shown Figures 10 and 11. As observed in the Figures, the non-mixing vane grid shows very little mixing with a steep temperature gradient between the hot rods and the cold rods. The mixing grid shows better mixing with a more uniform temperature distribution. Note that Figures 8 to 11 are displayed in different scales for better visual effects. When comparing to subchannel thermocouple measurements the temperature at the center of the subchannel was

selected in the CFD model. Figures 12 and 13 compare the test data at the exit to CFD and subchannel TH code [10] predictions indicating reasonable agreement. Discrepancies can be observed at the peripheral subchannels in the NMV case and this may be associated with large temperature gradients at these locations. Noticeable differences exist almost everywhere in the MV case. This indicates the limitation of applied turbulence model for the flow phenomenon (strong swirl prompted by mixing vanes) at this location.

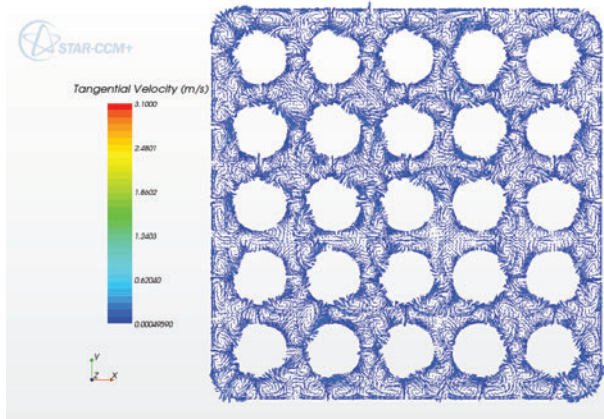


**Figure 8 Lateral Velocity at L/D ~1 Downstream of NMV Grid**

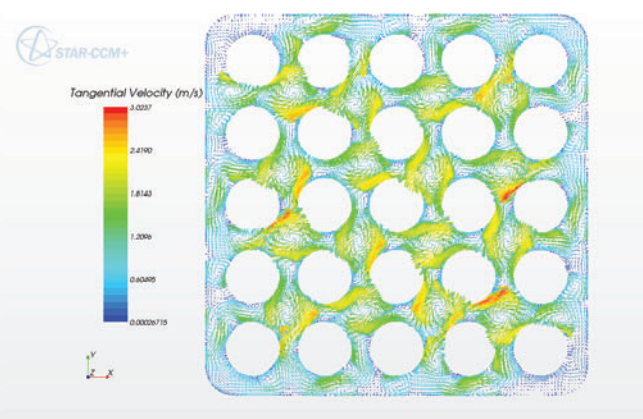


**Figure 9 Lateral Velocity at L/D ~1 Downstream of MV Grid**

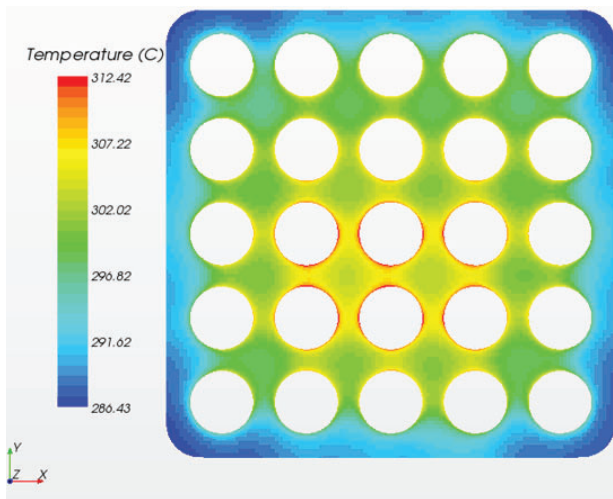


**Figure 10 NMV Grid Temperature Profile at Exit**

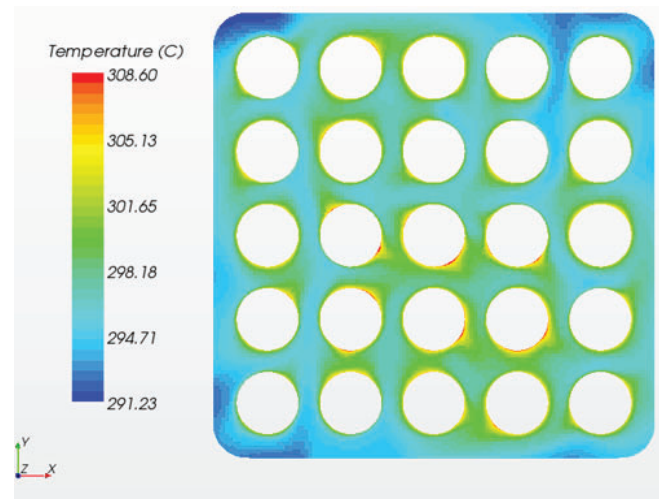


**Figure 11 MV Grid Temperature Profile at Exit**

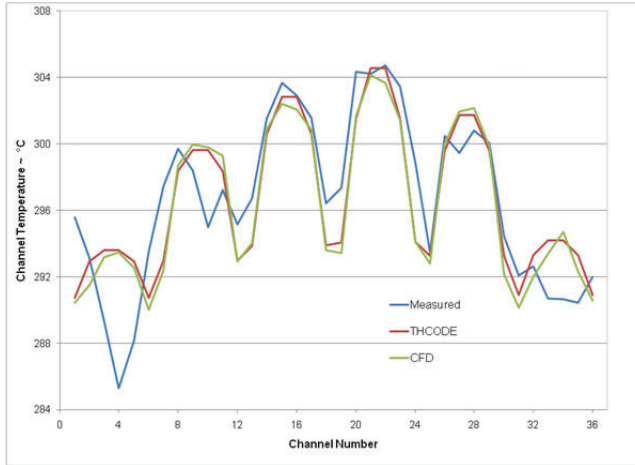


**Figure 12 Comparison of Subchannel TH Code and CFD Predictions to Test Data for NMV Grid**

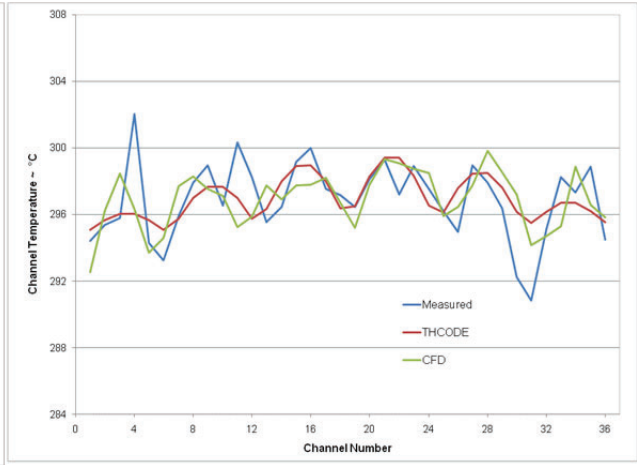


**Figure 13 Comparison of Suchannel TH Code and CFD Predictions to Test Data for MV Grid**

#### 4.2. Comparison of CFD predictions to LDV Measurements

Figure 14 shows the characteristic lateral velocity profile at approximately 1 hydraulic diameter downstream of the split mixing vane grid in the subchannel. This profile is compared to a CFD prediction with good agreement [2]. The overall conclusion deduced from the LDV tests and the CFD analysis suggests that the CFD tool can predict strong lateral velocity and swirl patterns just downstream of a mixing vane grid.

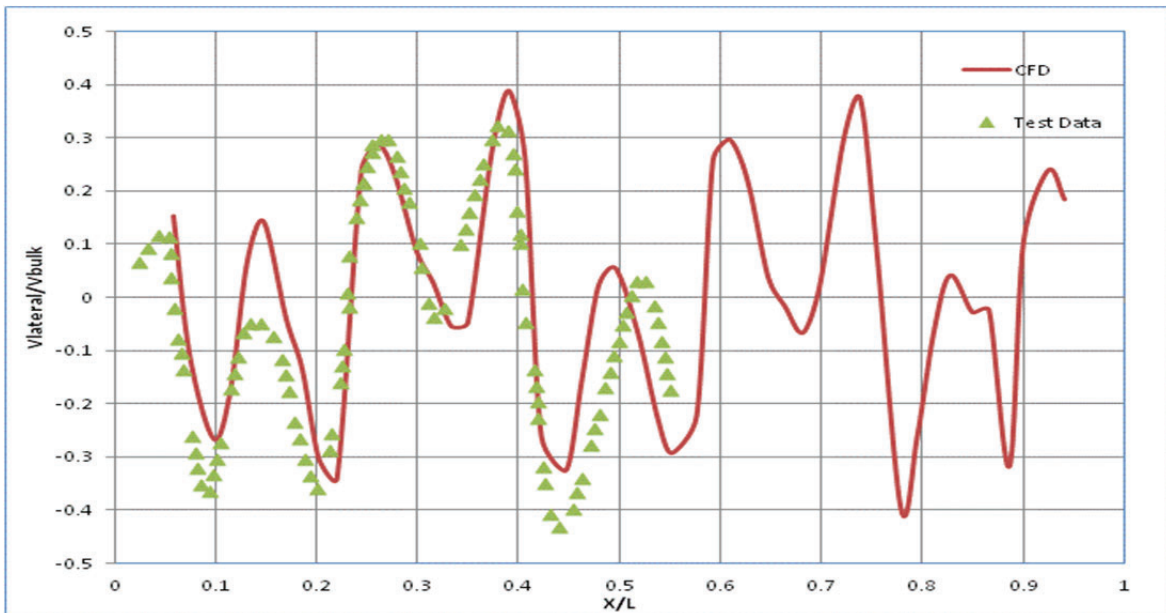


**Figure 14 LDV Lateral Velocity Profile Comparisons to CFD at Level A where X/L is distance from shroud wall**

### 4.3. Comparison of CFD Predictions to CHF Measurements

The reasonable agreement of the CFD tool to the single phase subchannel mixing and LDV test data provides some confidence the tool could be applied for CHF prediction (in other words, this is necessary, but may not be sufficient). Therefore, significant validation is still needed using two-phase data. Even though two-phase flow validation has not been made, a CFD prediction using available boiling models in Star-CCM+ was attempted to get an idea how the tool compares to available rod bundle CHF data and what gaps may exist to further improve models and predictions.

In the experiment, the onset of DNB was identified by monitoring the temperature of thermocouples. As the power gradually increases, when a sudden jump of temperature was observed, it was recorded as the DNB point and the corresponding CHF test power was recorded. Similarly, to capture the DNB point in a CFD simulation, the maximum temperature was monitored at the inner and outer surface of hot (high power) and cold (lower power) rods.

During a steady state simulation, the power (i.e., the heat flux specified at inner solid surfaces) was gradually increased in several steps. After converged or nearly-converged solutions were obtained at one power level, the power was increased to next level. When a sudden increase of monitored temperature happened, it was identified as the DNB point and the corresponding power level was recorded. The contour plots of steam volume fraction and dryout were then plotted at the rod outer surface. It can be seen that, when DNB happens, both the steam volume fraction and dryout increase dramatically.

Using the method outlined in Section 3 developed by Yan, et al [11],[12],[13] six cases were simulated using STAR CCM+ 7.06.012. For all cases, the DNB power captured by CFD simulation is at 85% of the actual DNB power recorded by experiment. Results for one of the mixing vane test runs are shown in Figure 15 where the maximum temperature is monitored. The jump in the monitored maximum temperature is believed to be the onset of DNB. Figure 16 shows the monitored surface integral of dryout at rod (including high power and low power rods) outer surfaces, which also shows a jump at the same iteration when the jump for monitored temperature happens. This is another indication for the onset of DNB. Note that actual DNB powers could be anywhere between the last two steps. Therefore, it is recommended using small power increments if a precise DNB power is desired.

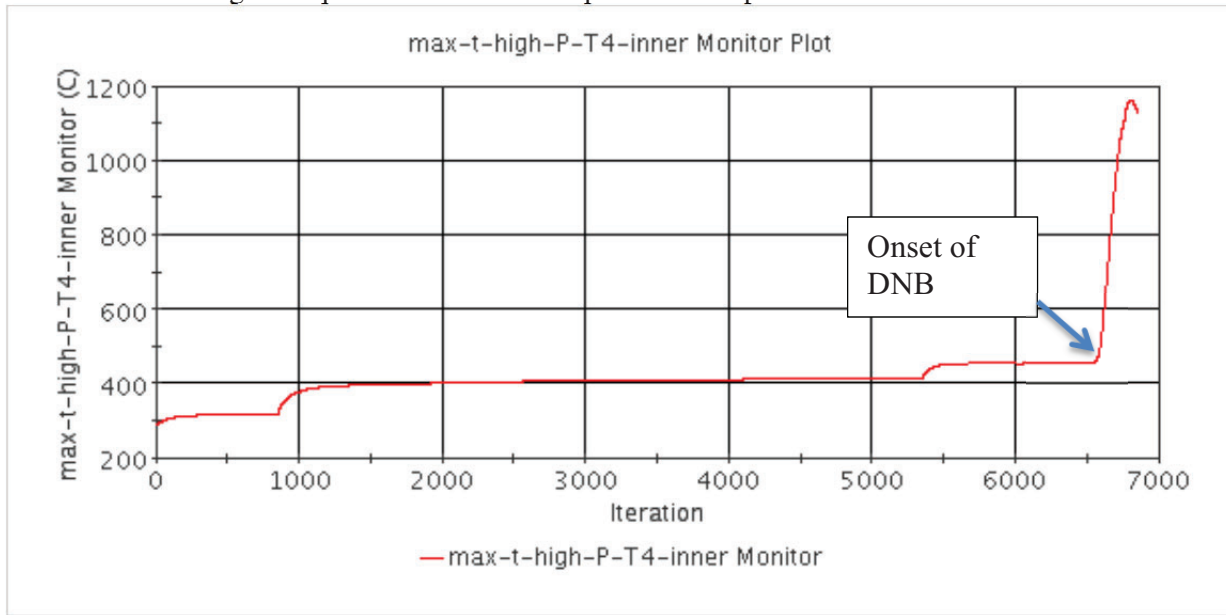
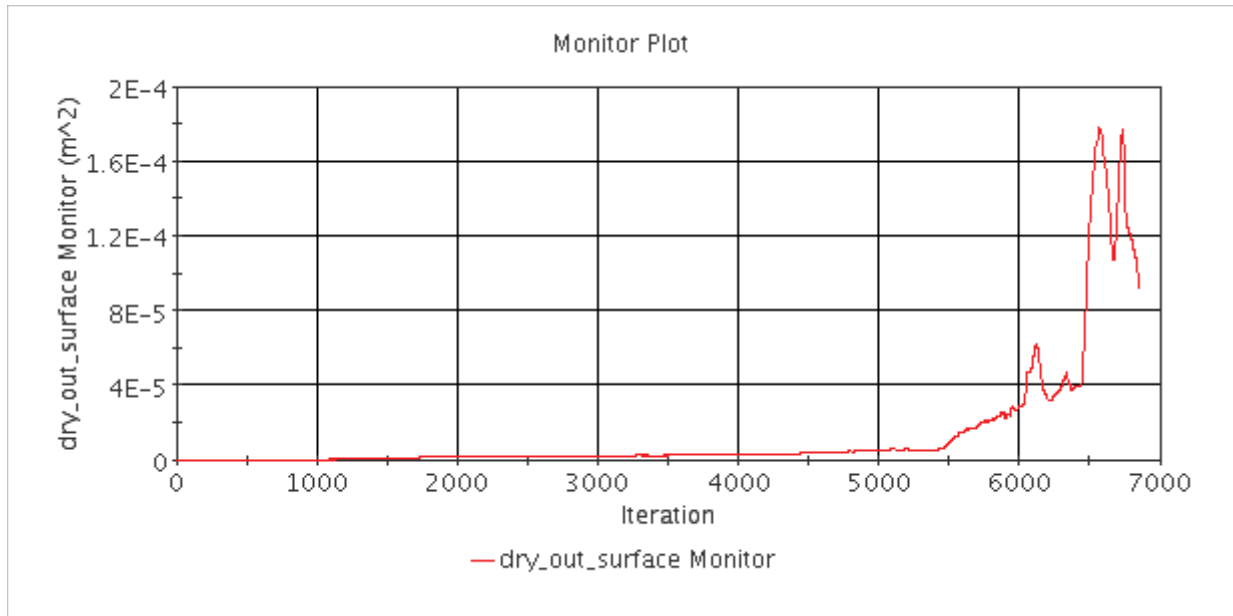
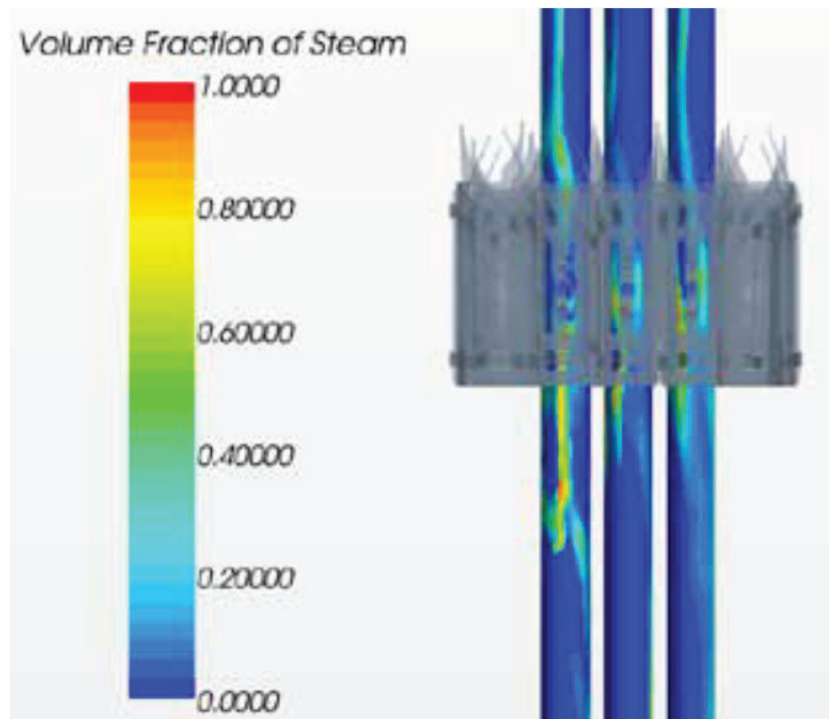


Figure 15 Maximum Temperature Monitored at Thermocouple Location



**Figure 16 Maximum Dryout Monitor at Rod Outer Surfaces**

Figures 17 and 18 show the contour plot for the steam volume fraction and dryout respectively, at rod outer surfaces (with last grid also presented). As can be seen from these figures, when DNB occurs, significant steam volume fraction and dryout present at the locations where DNB was observed in tests, indicating a possible change of boiling regime.



**Figure 17 Steam Volume Fraction at Rod Outer Surfaces**

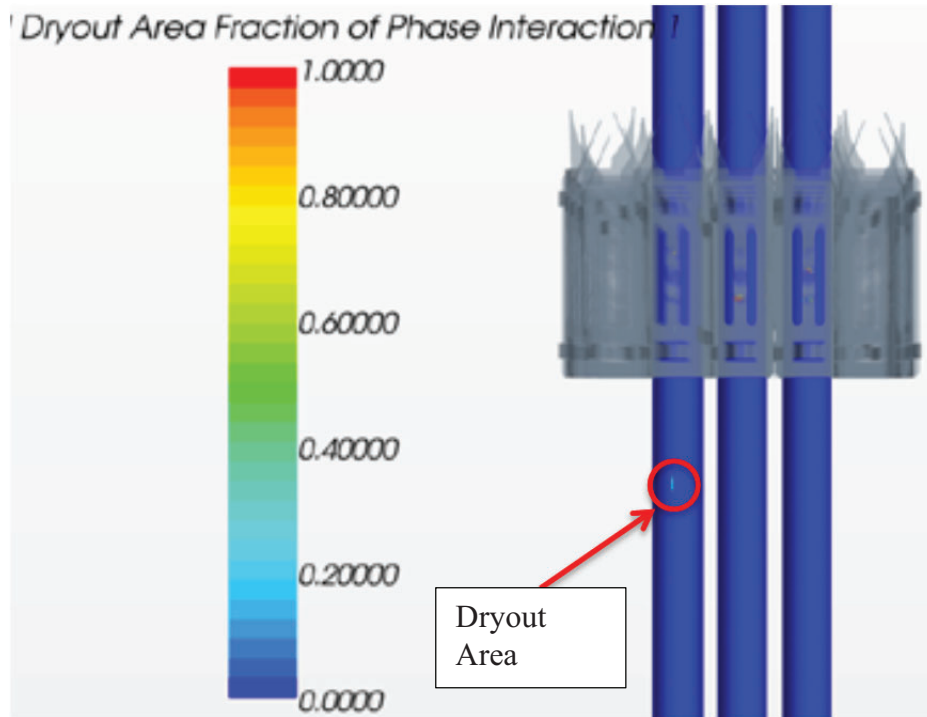


Figure 18 Dryout at Rod Outer Surface

Figure 19 shows the comparison of predicted CHF points with the test data for both non-mixing vane grid and mixing vane grid. The comparisons show that CFD predictions of CHF test power show a similar trend versus inlet temperature with the test data for the NMV and MV grids.

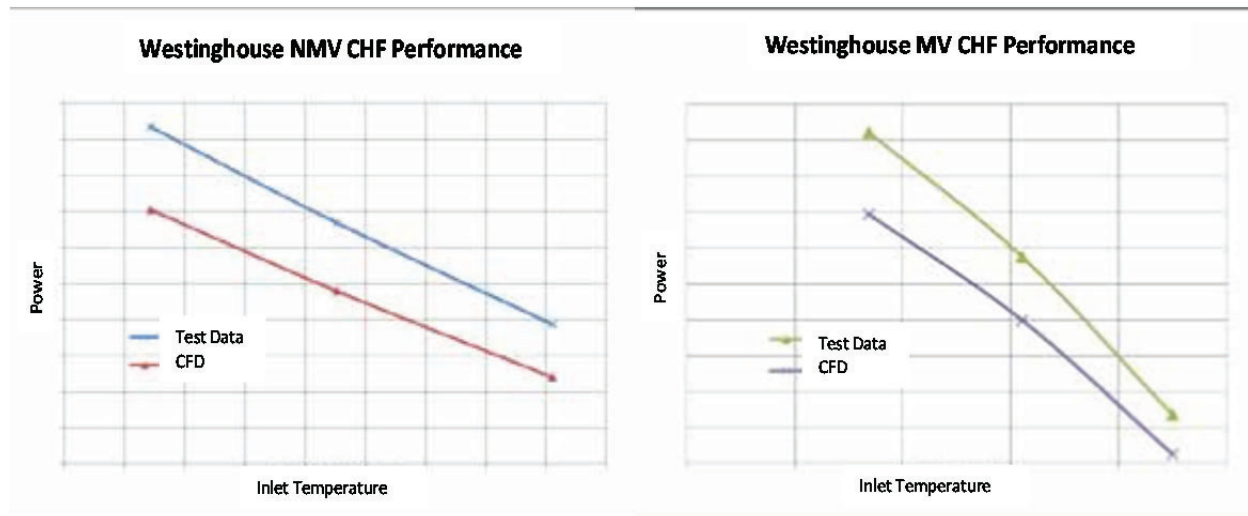


Figure 19 CFD Predicted and CHF Test Power Comparisons

## 5. CONCLUSIONS

To support validation, the CFD model results were first compared to single phase, exit subchannel temperature and LDV data from 5x5 rod bundle tests for two different spacer grid designs. Good agreement to data was observed in these comparisons indicating the CFD tool can produce reasonable results for two different spacer grid designs at single phase conditions.

After confirming the CFD tools make reasonable predictions for velocity profiles and exit subchannel temperatures, an approach to predicting CHF using the available two-phase flow boiling model in Star-CCM+ for the PWR rod bundle has been developed for comparison to CHF test data. The predicted CHF values show similar trends to the test data versus test operating conditions; however there are absolute differences that need to be further investigated and predictions are needed for a wide range of thermal hydraulic conditions. Further improvement of two-phase flow boiling models within the boundary layer of the fuel or heated rod wall is needed. Additional criteria of DNB occurrence in CFD simulations may be needed to single out false signals due to non-physical phenomena, such as numerical instabilities. Based on the existing modeling experiences, the prediction of CHF using a more mechanistic method in a CFD tool can be approached from two directions (or combination of both) where one requires modeling the detailed physics at the rod wall and the other direction is the benchmarking of the available CFD tools to the measured CHF for the rod bundle. The continued iteration of detailed model development and benchmarking for several different grid designs will hopefully result in a future validated approach for CHF prediction using CFD tools in PWR fuel design. Areas for continuous CFD code and modeling improvements for the CHF predictions include:

- Validity of the Eulerian-Eulerian two-phase flow with wall boiling model, such as partition wall boiling model at high pressure, high temperature and narrow channel applications,
- Bubble lift force modeling to account for bubble motion where velocity gradient is large or swirling flow exists,
- Interfacial area transport modeling to account for bubble dynamics (breakup or coalescence) and bubble size distribution,
- Uncertainties in mesh generation and numerical convergence criteria,
- Selection of DNB predictive parameters and criteria under different boiling heat transfer regimes,
- Selection of the boundary condition and location of such boundary condition with respect to the grid spacers.
- Impact of different turbulence models and options on CHF predictions.

## ACKNOWLEDGMENTS

The work performed by Drs. Jin Yan and Peng Yuan to apply CFD to rod bundle test data and developing the initial method for predicting CHF with CFD tools is greatly appreciated.

## REFERENCES

1. L. D., Smith, III, et al., "Benchmark Testing the ODEN CHF Loop To Columbia University HTRF," The 14th International Topical Meeting on Nuclear Reactor Thermal hydraulics, NURETH-14. Toronto, Ontario, Canada, September 25-30, 2011.
2. Z. E. Karoutas, P. F. Joffre, L. D. Smith III, J. Yan, J. Jiang, Y. Xu, P. Yuan, "Impact of Mixing Grid Design on Flow Patterns and CHF Performance", LWR Fuel Performance TopFuel Meeting, September 15-19, 2013, Charlotte, NC.
3. STAR-CCM+ by CD-adapco, [http://www.cd-adapco.com/products/STAR-CCM\\_plus/index.html](http://www.cd-adapco.com/products/STAR-CCM_plus/index.html)

4. S. Lo and J. Osman, "CFD Modeling of Boiling Flow in PSBT 5×5 Bundle"; Science and Technology of Nuclear Installations, Volume 2012 (2012), Article ID 795935, 8 pages, doi:10.1155/2012/795935
5. A. Tomiyama, I. Kataoka, I. Zun, T. Sakaguchi , "Drag coefficients of single bubbles under normal and micro gravity conditions", JSME International Journal, Series B, 41 (2), pp. 472-479, 1998.
6. M. Lemmert and J. M. Chawla. Influence of flow velocity on surface boiling heat transfer coefficient. Heat Transfer in Boiling, E. Hahne and U. Grigull (Eds.), Academic Press and Hemisphere 1977, ISBN 0-12-314450-7, pages 237–247, 1977.
7. V. I. Tolubinsky, D. M. Kostanchuk, "Vapour Bubbles Growth Rate and Heat Transfer Intensity at Subcooled Water Boiling Heat Transfer", 4th International Heat Transfer Conference, Paris, vol. 5, Paper No. B-2.8 (1970).
8. N. Kurul and M. Z. Podowski, "Multidimensional effects in sub-cooled boiling," Proc. of 9th Heat Transfer Conference, Jerusalem, 1990.
9. Z. E. Karoutas, J. Yan, P. F. Joffre, P. Yuan, "Prediction of Subchannel Mixing Downstream of Spacer Grids", Proceedings of ICAPP2014 Charlotte, NC. April 6-9, 2004, Paper 14357.
10. "TORC Code, A Computer Code for Determining the Thermal Margin of a Reactor Core", CENPD-161-NP-A, April 1986 Combustion Engineering, Inc.
11. J. Yan et al, "Evaluating Spacer Grid CHF Performance by High Fidelity 2-Phase Flow Modeling," LWR Fuel Performance Meeting TopFuel 2013, Paper 8348, Charlotte, NC, September 15-19, 2013.
12. J. Yan, , L. D. Smith III, Z. Karoutas, "Departure from Nucleate Boiling Modeling Development for PWR Fuel", Proceedings of the 2013 21st International Conference on Nuclear Engineering, ICONE21, July 29- August 2, 2013, Chengdu, China
13. J. Yan, P. Yuan, P. F. Joffre, Z. E. Karoutas, L. D. Smith III, "CHF Model Development in Westinghouse", International seminar on Subchannel Analysis CFD modeling and verification, CHF experiment and benchmarking ISACC-2013 August 03-04, 2013, Xian, China
14. L. A. Gilman, "Development of a General Purpose Subgrid Wall Boiling Model from Improved Physical Understanding for Use in Computational Fluid Dynamics" DOCTOR OF PHILOSOPHY IN NUCLEAR SCIENCE AND ENGINEERING AT THE MASSACHUSETTS INSTITUTE OF TECHNOLOGY, June 2014.